

Measurements of MRI R2* Relaxation Rate in Liver and Muscle: Animal Model

Chiung-Yun Chang, Po-Chou Chen, Jiun-Shiang Tzeng, Ka-Wai Mac, Chia-Chi Hsiao, Jo-Chi Jao

Abstract—This study was aimed to measure effective transverse relaxation rates (R2*) in the liver and muscle of normal New Zealand White (NZW) rabbits. R2* relaxation rate has been widely used in various hepatic diseases for iron overload by quantifying iron contents in liver. R2* relaxation rate is defined as the reciprocal of T2* relaxation time and mainly depends on the constituents of tissue. Different tissues would have different R2* relaxation rates. The signal intensity decay in Magnetic resonance imaging (MRI) may be characterized by R2* relaxation rates. In this study, a 1.5T GE Signa HDxt whole body MR scanner equipped with an 8-channel high resolution knee coil was used to observe R2* values in NZW rabbit's liver and muscle. Eight healthy NZW rabbits weighted 2 ~ 2.5 kg were recruited. After anesthesia using Zoletil 50 and Rompun 2% mixture, the abdomen of rabbit was landmarked at the center of knee coil to perform 3-plane localizer scan using fast spoiled gradient echo (FSPGR) pulse sequence. Afterwards, multi-planar fast gradient echo (MPFGR) scans were performed with 8 various echo times (TEs) to acquire images for R2* measurements. Regions of interest (ROIs) at liver and muscle were measured using Advantage workstation. Finally, the R2* was obtained by a linear regression of $\ln(SI)$ on TE. The results showed that the longer the echo time, the smaller the signal intensity. The R2* values of liver and muscle were $44.8 \pm 10.9 \text{ s}^{-1}$ and $37.4 \pm 9.5 \text{ s}^{-1}$, respectively. It implies that the iron concentration of liver is higher than that of muscle. In conclusion, the more the iron contents in tissue, the higher the R2*. The correlations between R2* and iron content in NZW rabbits might be valuable for further exploration.

Keywords—Liver, MRI, multi-planar fast gradient echo, muscle, R2* relaxation rate.

I. INTRODUCTION

INCREASED iron deposition is known to be associated with other systemic disorders, including hepatitis, hepatic fibrosis, hepatic cirrhosis and tumor [1]–[3]. A non-invasive method to detect iron deposition would be appreciated. Magnetic resonance imaging (MRI) has no ionizing radiation and can provide images with high contrast among tissues. Therefore, MRI has become a very important modality in clinical diagnosis. Furthermore, the powerful part is that MRI provide multi-parameters for tissue characterization, e.g. proton density,

longitudinal relaxation time (T1), and transverse relaxation time (T2) etc. MRI was used in detecting hepatic iron overload in patients with cirrhosis of different origins. It suggested that MR imaging technique might play an important role in detection of hepatic iron overload in liver diseases [2]. Effective transverse relaxation rate (R2*) is defined as the reciprocal of effective transverse relaxation time (T2*). T2* is associated with T2 values and field inhomogeneity. T2* is usually lower than T2. R2* imaging techniques were used to study and compare iron burden between 3T and 1.5T MR scanners. It was found that R2* relaxation rates of patients who suffering systemic disorders were higher than those of normal volunteers [3]. The gold standard for hepatic iron quantification is core liver biopsy [4]; however, this procedure is relatively invasive, difficult to repeat, and limited by sampling error. MRI is noninvasive and good for iron overload detection.

Noninvasive techniques for hepatic iron evaluation include superconducting quantum interference devices (SQUIDs) [5] and magnetic resonance imaging (MRI). SQUID is a kind of special equipment, which cannot be widely used in clinic [6]. Magnetic-susceptibility effects were studied for human iron stores [5]. Abnormal iron accumulation in tissues and organs can be found in numerous diseases. MRI R2* relaxation rates have been used in various hepatic diseases for iron overload by quantifying iron contents in liver [1]. MR R2* technique can be used to rapidly assess iron contents in the septum of heart as well. In addition, R2* imaging technique was used to perform for a longitudinal follow-up study to investigate the progression of Parkinson's disease. It was concluded that R2* relaxation rate might act as a biomarker for the progression of Parkinson's disease [7]. Furthermore, MRI R2 and R2* mapping was used to evaluate the accuracy of hepatic iron concentration in transfusion-dependent thalassemia and sickle cell disease patients [8].

The R2* relaxation rate conveys the magnetic susceptibility effects due to reversible and irreversible contribution of iron [9]. Gradient-echo pulse sequence are commonly used to measure the R2* relaxation rates. There is strong correlation between R2* values and iron concentrations. R2* could be affected by both reversible and irreversible iron effects. Therefore, R2* can be characterized as an imaging biomarker because it has high sensitivity to iron contents [7]. The R2* relaxation rates of different tissues are various due to their different constituents, for example, R2* relaxation rate of liver is higher than that of heart [3]. The signal intensity decay in MRI may be characterized by R2* relaxation rates. Animal MRI models are known to be essential for translational researches. The aim of this study was to measure R2* relaxation rates of New Zealand

Chiung-Yun Chang, Jiun-Shiang Tzeng, Ka-Wai Mac are with the Department of Medical Imaging and Radiological Sciences, Kaohsiung Medical University, Taiwan, R.O.C. (e-mail: judy00912@gmail.com, q123294@hotmail.com, winnie_abc@yahoo.com.hk).

Po-Chou Chen is with the Department of Biomedical Engineering, I-SHOU University, Taiwan, R.O.C. (e-mail: pcchen@isu.edu.tw).

Chia-Chi Hsiao is with the department of Radiology, Kaohsiung Veterans General Hospital, Taiwan, R.O.C. (e-mail: cchsiao@vghks.gov.tw).

Jo-Chi Jao is with the department of Medical Imaging and Radiological Sciences, Kaohsiung Medical University, Taiwan, R.O.C. (corresponding author, phone: 886-7-3121101 ext. 2356; fax: 886-7-3113449; e-mail: jochja@kmu.edu.tw).

(NZW) rabbit's liver and muscle.

II. MATERIALS AND METHODS

A. Animal Model

Eight healthy NZW rabbits weighted 2 ~ 2.5 kg were used in this experiment. These rabbits were raised under controlled environmental conditions. Temperature and humidity were controlled at 21-23° and 48~62%, respectively. The 12-hour day-night cycle was 7 AM to 7 PM and 7 PM to 7 AM. The work was conducted with the affidavit of animal use protocol approved by the Institutional Animal Care and Use Committee of I-Shou University (IACUC-ISU-102005).



Fig. 1 The positioning of a NZW rabbit

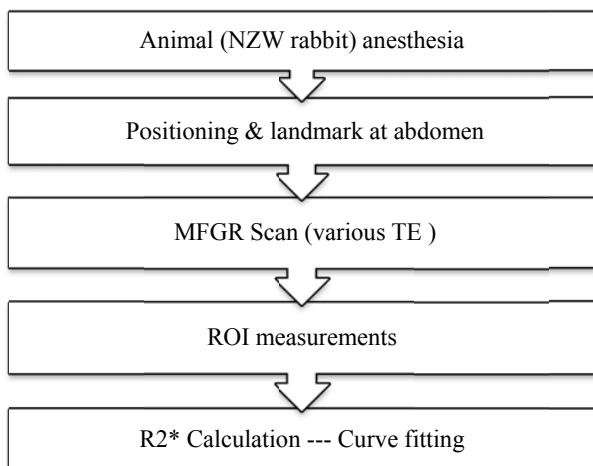


Fig. 2 The flowchart of R2* measurements

B. Imaging Protocol

NZW rabbits were sedated with Zoletil 50 and Rompun 2% mixture (0.9 ml/kg) via intramuscular injection before scanning. All examinations were performed using a 1.5T MRI system (GE Signa HDxt whole body MR scanner) and an 8-channel high resolution knee coil. All images were acquired in transverse planes. Each rabbit was in the supine position and wore a corset to reduce breathing artifacts (Fig. 1). After the NZW rabbit's abdomen was positioned at the center of the knee coil, multi-slice axial, coronal and sagittal images were

obtained for selecting the slices of interest using the fast spoiled gradient echo (FSPGR) pulse sequence. Then, multi-planar fast gradient echo (MPFGR) pulse sequence was used to acquire images for R2* calculations using various echo times (TEs). In order to increase the accuracy of R2* measurements, eight various TEs were used in this study. The scanning parameters were TR (repetition time) = 100 ms, TE = 2/4/6/8/10/12/14/16 ms, FA (flip angle) = 80°, FOV (field of view) = 18 × 18 cm², BW (bandwidth) = 62.5 kHz, matrix = 96 × 96, NEX (number of excitations) = 1, number of slice = 40, and slice thickness = 5 mm. The flowchart of this experiment for R2* measurements is shown in Fig. 2.

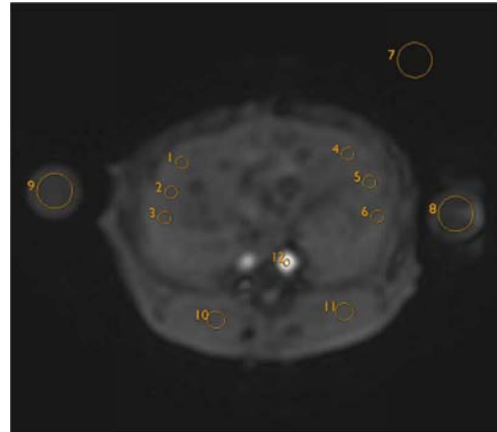


Fig. 3 A demonstration of ROIs measurement

C. Theoretical Approach

The MR signal Intensity can be expressed as (1),

$$SI = M_0 \times (1 - e^{-\frac{TR}{T_1}}) \times e^{-\frac{TE}{T_2^*}}, \quad (1)$$

where M_0 is the net magnetization, $(1 - e^{-\frac{TR}{T_1}})$ is namely T1 term and $e^{-\frac{TE}{T_2^*}}$ is namely T2* term. It can be shortly formulated as (2) because the T1 term of MR Signal intensity (SI) can be integrated with M_0 becomes M as the repetition time was fixed throughout the whole experiments.

$$SI = M \times e^{-\frac{TE}{T_2^*}} \quad (2)$$

The logarithmic of measured MR signal intensity can be expressed as,

$$\ln(SI) = \ln M - \frac{TE}{T_2^*} \quad (3)$$

It can be further substitute R2* in (2) as R2* is the reciprocal of T2* relaxation time.

$$\ln(SI) = \ln M - TE \times R2^* \quad (4)$$

Clearly, (3) showed a linear relationship between $\ln(SI)$ and R2*. It confirms that R2*s of liver and muscle can be obtained by a linear regression of $\ln(SI)$ on TE.

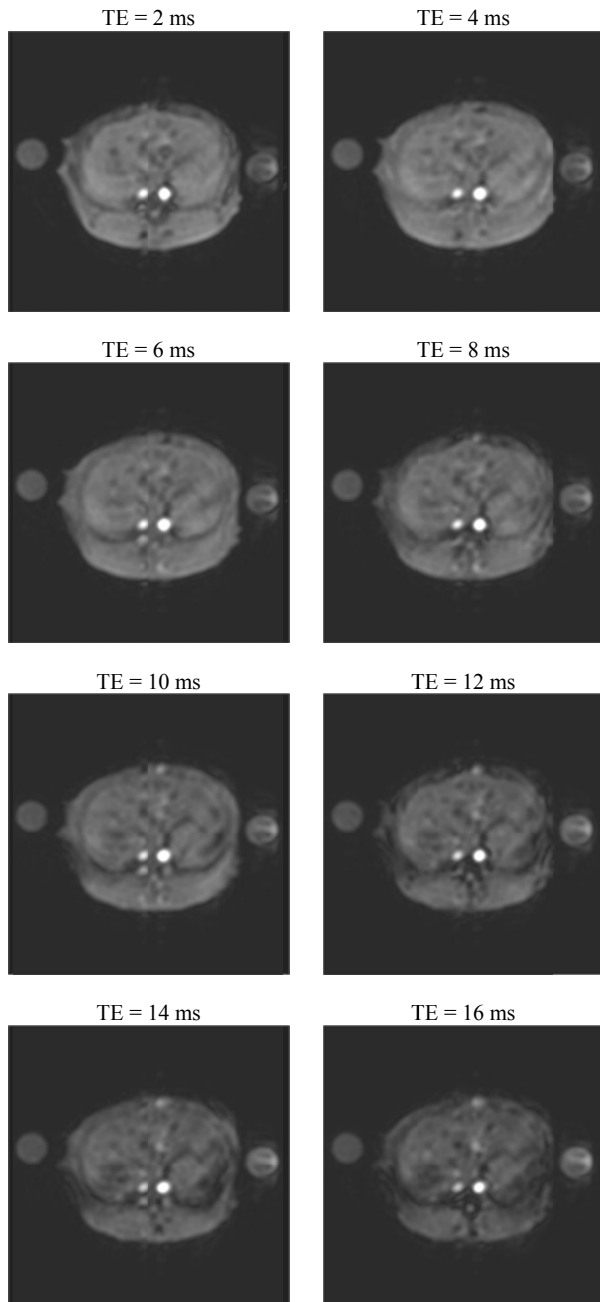


Fig. 4 MRI liver images with different TEs

D. Image Analysis

Regions of interest (ROIs) were measured using Advantage workstation. ROI 1-6 were circled at liver and all visible vessels were avoided, where ROI 7 was at background; ROI 8-9 were at muscle (Fig. 3). Six $R2^*$ ROI values of liver and two ROI values of muscle were averaged to improve the accuracy of tissue $R2^*$.

E. Statistical Analysis

Microsoft Excel 2010 was used for statistical analysis. $R2^*$ values of liver and muscle were obtained by a linear regression

of $\ln(SI)$ on TE.

III. RESULTS

Fig. 4 shows MR liver images obtained from MFGR pulse sequence with different TEs. There are no respiratory artifacts found in MFGR images. Fig. 5 shows signal intensity curves of NZW rabbit's liver and muscle versus TE obtained after measurements of ROIs. The results showed that the longer the TE, the smaller the signal intensity. Then, the logarithmic of signal intensity curves of liver and muscle versus TE are shown in Fig. 6.

The calculated $R2^*$ values of liver and muscle were $44.8 \pm 10.9 \text{ s}^{-1}$ and $37.4 \pm 9.5 \text{ s}^{-1}$, respectively (Fig. 7).

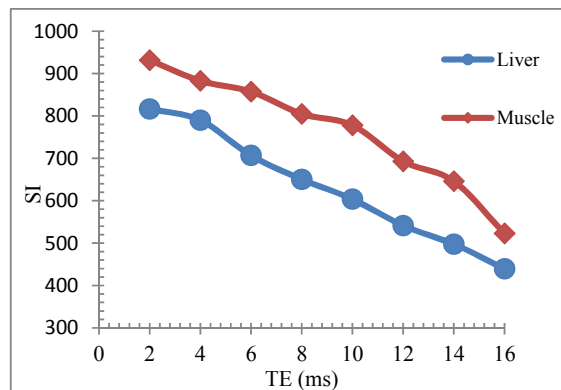
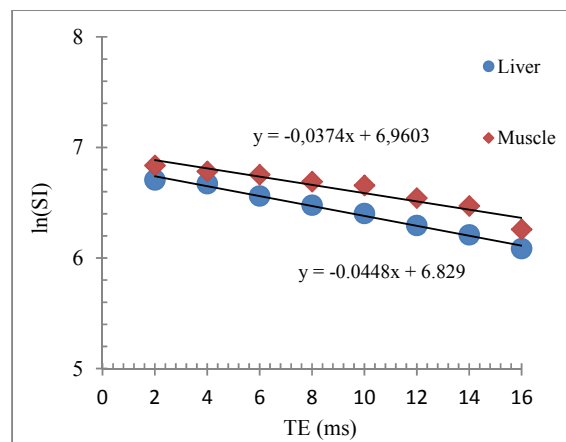


Fig. 5 MR signal intensity (SI) of liver and muscle versus TE

Fig. 6 The logarithmic of MR signal intensity, $\ln(SI)$, versus TE with linear regression.

IV. DISCUSSION AND CONCLUSIONS

$R2^*$ values were obtained from images with various TE values. Totally eight different TE values were adopted to obtain $R2^*$ values using a linear regression method in this experiment. The experimental results showed that the signal intensity of the liver and muscle decreased as TE increased. $R2^*$ values of liver are higher than those of muscle. It implies that liver has more iron contents than muscle does. Ferritin complexes are presented in all cells, but commonly present in bone marrow,

liver and spleen. The liver's stores of ferritin are the primary physiologic source of reserved iron in the body. Thus, it might be associated with iron contents in tissues. The experimental results imply the feasibility of quantifying liver iron by the use of MR $R2^*$ relaxometry. In conclusion, $R2^*$ values were positively correlated with iron concentration in tissue. The quantitative correlations between $R2^*$ and iron concentration of NZW rabbits might be valuable for further exploration.

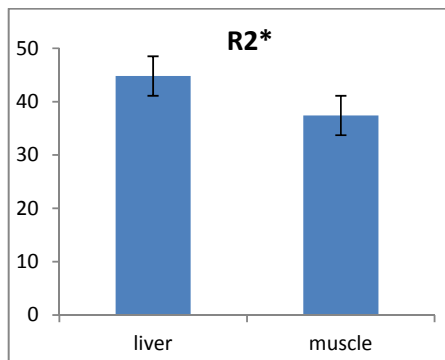


Fig. 7 $R2^*$ values of liver and muscle

ACKNOWLEDGMENT

The authors would like to thank the financial support of the NSC in Taiwan, R.O.C. (Grant No. NSC 99-2221-E-214-008)

REFERENCES

- [1] R. P. Lim, K. Tuvia, C. H. Hajdu, M. Losada, R. Gupta, T. Parikh, J. S. Babb, B. Taouli, "Quantification of hepatic iron deposition in patients with liver disease: comparison of chemical shift imaging with single echo T2*-weighted imaging," *AJR Am J Roentgenol*, vol. 194, no. 5, 1288-1295, May 2010.
- [2] E. Szurowska, K. Sikorska, E. Izzycka-Swieszewska, T. Nowicki, T. Romanowski, K. P. Bielawski, M. Studniarek, "The role of MR imaging in detection of hepatic iron overload in patients with cirrhosis of different origins," *BMC Gastroenterol*, vol. 10, 13, 2010.
- [3] P. Storey, A. A. Thompson, C. L. Carqueville, J. C. Wood, R. A. de Freitas, C. K. Rigsby, "R2* imaging of transfusional iron burden at 3T and comparison with 1.5T," *Magn Reson Imaging*, vol. 25, no. 3, pp. 540-547, Mar. 2007.
- [4] M. Barry, S. Sherlock, "Measurement of liver-iron concentration in needle-biopsy specimens," *Lancet*, vol. 1, no. 7690, pp. 100-103, Jan. 1971.
- [5] G. M. Brittenham, D. E. Farrell, J. W. Harris, E. S. Feldman, E. H. Danish, W. A. Muir, J. H. Tripp, E. M. Bellon, "Magnetic-susceptibility measurement of human iron stores," *N Engl J Med*, vol. 307, pp. 1671-1675, Dec. 1982.
- [6] E. Angelucci, G. Barosi, C. Camaschella, M. D. Cappellini, M. Cazzola, R. Galanello, M. Marchetti, A. Piga, S. Tura, "Italian Society of Hematology practice guidelines for the management of iron overload in thalassemia major and related disorders," *Haematologica*, vol. 93, no. 5, pp. 741-752, May. 2008.
- [7] M. Ulla, J. M. Bonny, L. Ouchchane, I. Rieu, B. Claise, F. Durif, "Is R2* a new MRI biomarker for the progression of Parkinson's disease? A longitudinal follow-up," *PLoS One*, vol. 8, no. 3, pp. e57904, Mar. 2013.
- [8] J. C. Wood, C. Enriquez, N. Ghugre, J. M. Tyzka, S. Carson, M. D. Nelson, T. D. Coates, "MRI R2 and R2* mapping accurately estimates hepatic iron concentration in transfusion-dependent thalassemia and sickle cell disease patients," *Blood*, vol. 106, no. 4, pp. 1460-1465, Aug. 2005.
- [9] J. Ma, F. W. Wehrli, "Method for image-based measurement of the reversible and irreversible contribution to the transverse-relaxation rate," *J Magn Reson B*, vol. 111, no. 1, pp. 61-69, Apr. 1996.